

Received: 2018.02.25  
Accepted: 2018.05.14  
Published: 2018.06.02

# MicroRNA-365 Inhibits Cell Growth and Promotes Apoptosis in Melanoma by Targeting BCL2 and Cyclin D1 (CCND1)

Authors' Contribution:  
Study Design A  
Data Collection B  
Statistical Analysis C  
Data Interpretation D  
Manuscript Preparation E  
Literature Search F  
Funds Collection G

ABDEF 1 **Yong Zhu**  
BCF 2 **Xing Wen**  
ABEF 3 **Peng Zhao**

1 Department of Stomatology, Xi'an Medical University, Xi'an, Shaanxi, P.R. China  
2 Department of Stomatology, Xi'an Gao Xin Hospital, Xi'an, Shaanxi, P.R. China  
3 Oncology Ward Three, Tang Du Hospital, Xi'an, Shaanxi, P.R. China

**Corresponding Author:** Yong Zhu, e-mail: zhuyong@xjy.edu.cn

**Source of support:** This work was supported by grants from the Support Project for Key Construction Discipline of Clinical Science of Stomatology in Xi'an Medical University

**Background:** MicroRNA-365 (miR-365) is involved in the development of a variety of cancers. However, it remains largely unknown if and how miRNAs-365 plays a role in melanoma development.

**Material/Methods:** In this study, we overexpressed miR-365 in melanoma cell lines A375 and A2058, via transfection of miR-365 mimics oligos. We then investigated alterations in a series of cancer-related phenotypes, including cell viability, cell cycle, apoptosis, colony formation, and migration and invasion capacities. We also validated cyclin D1 (CCND1) and BCL2 apoptosis regulator (BCL2) as direct target genes of miR-365 by luciferase reporter assay and investigated their roles in miR-365 caused phenotypic changes. To get a more general view of miR-365's biological functions, candidate target genes of miR-365 were retrieved via searching online databases, which were analyzed by Gene Ontology (GO) and Kyoto Encyclopedia of Genes and Genomes (KEGG) pathway enrichment analyses for potential biological functions. We then analyzed The Cancer Genome Atlas (TCGA) Skin Cutaneous Melanoma (SKCM) dataset for correlation between miR-365 level and clinicopathological features of patients, and for survival of patients with high and low miR-365 levels.

**Results:** We found that miR-365 was downregulated in melanoma cells. Overexpression of miR-365 remarkably suppressed cell proliferation, induced cell cycle arrest and apoptosis, and compromised the migration and invasion capacities in A375 and A2058 cell lines. We also found that the phenotypic alterations by miR-365 were partially due to downregulation of CCND1 and BCL2 oncogenes. The bioinformatics analysis revealed that predicted targets of miR-365 were widely involved in transcriptional regulation and cancer-related signaling pathways. However, analysis of SKCM dataset failed to find differences in miR-365 level among melanoma patients at different clinicopathologic stages. The Kaplan-Meier analysis also failed to discover significant differences in overall survival and disease-free survival between patients with high and low miR-365 levels.

**Conclusions:** Our findings suggested that miR-365 might be an important novel regulator for melanoma formation and development, however, the *in vivo* roles in melanoma developments need further investigation.

**MeSH Keywords:** **Apoptosis • bcl-Associated Death Protein • Cyclin D1 • Melanoma • MicroRNAs**

**Full-text PDF:** <https://www.medscimonit.com/abstract/index/idArt/909633>

 3928

 4

 6

 33



## Background

Melanoma, a skin malignancy notorious for its aggressiveness and high metastatic potential, has had a fast increase in its incidence rate, and accounts for over 65% of skin cancer-related deaths [1,2]. Most localized melanomas are curable with surgical resection, while the prognosis of patients with distant metastases is usually poor with a 10-year survival rate of only 16%, mainly due to innate or acquired resistance to therapeutic regimens [3]. This situation highlights the significance of further understanding of the underlying molecular mechanisms that contribute to melanoma development and metastasis.

MicroRNAs (miRNAs) are small non-coding RNAs that negatively regulate gene expression post-transcriptionally by pairing to the 3'-untranslated region (3'-UTR) of target mRNAs [4,5]. miRNAs are involved in regulating a series of cellular functions, including development, differentiation, apoptosis, and proliferation. Deregulated miRNA expression has been shown to contribute to the development of cancers, including breast cancer [6], digestive tract cancers [7], melanoma [5], and so forth. miR-365 is located on chromosome 16p13.12, a region that has been involved in multiple oncogenic processes. The expression pattern and biological roles of miR-365 are cancer type-dependent. miR-365 is highly expressed in cutaneous squamous cell carcinoma [8,9] and breast cancer [10], while it is downregulated in colon cancer [11], lung cancer [12], and melanoma [13]. miR-365 may display either a pro-proliferative or pro-apoptotic role in a specific cancer type. The roles of miR-365 in melanoma development is very poorly understood. Bai et al. have shown that miR-365 was downregulated in melanoma tissues and ectopic expression of miR-365 suppressed cell cycle progression and promoted apoptosis by targeting NRP1, which is an essential regulator of cell migration and invasion, suggesting that miR-365 exerted a tumor-suppressive effect in melanoma [13].

Cyclin D1 (CCND1) is a member of the cyclins, which are essential in regulating cell cycle [14]. *CCND1* is a well-established human oncogene [14], which is commonly overexpressed in different types of cancers such as breast cancer [15], lung cancer [16], and melanoma [17]. *CCND1* overexpression can result in a number of potentially oncogenic effects and have been shown associated with poor patient outcome [18]. BCL2 apoptosis regulator (BCL2) belongs to the BCL2 family proteins, which are important regulators of apoptosis [19]. Antiapoptotic BCL2 family members, including BCL2, BCLXL, MCL1, and BCLW, inhibit apoptosis by sequestering the activators from interacting with BAX and BAK [20]. Overexpression of anti-apoptotic *BCL2* has been observed in many types of cancers, such as follicular lymphoma [21], breast cancer [22], prostate cancers [23] and melanoma [24]. Upregulated expression of BCL2 protein promotes tumorigenesis and tumor progression and is associated with poor patient prognosis [25]. *CCND1* and *BCL2* have

been reported as targets genes of miR-365 in colon cancer [11]. Thus, in this study we investigated the functional relationship between miR-365 and these 2 genes.

In this study, to further explore the roles of miR-365 in melanoma development and reveal the underlying molecular mechanisms, we investigated the effects of miR-365 overexpression on cell cycle, apoptosis, cell migration and invasion in 2 melanoma cell lines, A375 and A2058. We also investigated the roles of CCND1 and BCL2 in the cellular effects of miR-365. To obtain a comprehensive understanding of the potential biological functions of miR-365, the Gene Ontology (GO) analysis and Kyoto Encyclopedia of Genes and Genomes (KEGG) pathway enrichment analysis of predicted targets of miR-365 were carried out. In addition, analysis of the The Cancer Genome Atlas (TCGA) datasets for melanoma patients was also performed to investigate the association between miR-365 level and the clinicopathologic features and outcomes of melanoma patients.

## Material and Methods

### Cell culture

NHEM (Normal Human Epidermal Melanocytes) cell line was obtained from Miao Tong Biological Technology (Shanghai, China) and cultured in M2 medium. The human melanoma cell lines A375, A2058, SK-MEL-2, and SK-MEL-28 were obtained from China Center for Type Culture Collection (Wuhan, China). These cell lines were cultured in Dulbecco's modified Eagle's medium (DMEM) supplemented with 10% fetal bovine serum. All cell lines were incubated at 37°C with 5% CO<sub>2</sub> in a humidified atmosphere.

### Transfection of miR-365 mimics

To transiently overexpress miR-365, A375 and A2058 cells were transfected with miR-365 mimic oligos (Life Technologies, USA) at a final concentration of 100 nM by using lipofectamine 2000 (Thermo Fisher Scientific, USA) according to the manufacturer's instructions. The control cells were transfected with the non-targeting control oligo (NC oligo for short, Life Technologies, USA) at the same concentration.

### Quantitative real-time-PCR

Total RNA, including miRNA, was extracted from cells using the miRNeasy mini kit (Qiagen, USA) according to manufacturer's instructions. For measuring BCL2 and CCND1 mRNA levels, 1.5 µg total RNA was reversely transcribed into cDNA using the Omniscript RT kit (Qiagen, USA) according to manufacturer's instructions. The qRT-PCR was then performed to detect the levels of BCL2 and CCND1 as described by literature [26]. Briefly, 2 µL of cDNA (diluted in 1: 10) was used as templates

for qRT-PCR using the iQ SYBR Green Supermix (Bio-Rad, USA) on a CFX Real-Time PCR Detection System (Bio-Rad, USA). The amplification protocol is as following: 95°C for 3 min; followed by 35 cycles of 95°C for 15 sec and 60°C for 30 sec. GAPDH was used as an internal control. Primer sequences are as follows: GAPDH forward: 5'-AAGCCTGCCGGTACTAAC-3' and reverse: 5'-GGGCCCAATACGACCAAA-3'; BCL-2 forward: 5'-ATGTGTGTGGA GAGCGTCAA-3' and reverse: 5'-GGGCCGTACAGTCCACAAA-3'; CCND1 forward: 5'-CAGATCATCCGCAAACACGC-3' and reverse: 5'-AAGTTGTTGGGCTCCTCAG-3'. All reactions were performed in triplicate. Fold changes in mRNA expression levels were calculated using the  $2^{-\Delta\Delta CT}$  method [27]. For measuring miR-365 levels, a miScript II RT kit (Qiagen, USA) was used to convert miRNAs to cDNA and to add a universal tag to each cDNA product. The levels of miR-365 was detected via performing qRT-PCR assay using the miScript SYBR Green PCR kit (Qiagen, USA) according to the following protocol: 95°C for 15 min, followed by 40 cycles of 94°C for 15 sec, 55°C for 30 sec, and 70°C for 30 sec [28]. The qRT-PCR primers for miR-365 was 5'-GCTAATGCCCTAAAAATCC-3'. U6 primer was 5'-GAACGATACAGAGAAGATTAGCA-3'. All reactions were performed in triplicate. The expression level of miR-365 was normalized to that of U6 snRNA. Fold changes in miR-365 levels were calculated using  $2^{-\Delta\Delta CT}$  method [27].

#### MTT assay

Cell viability was measured by using a 3-(4,5-dimethylthiazol-2-yl)-2,5-diphenyltetrazolium bromide (MTT) assay (Sigma, USA) as described in published study [29]. Briefly, cells were seeded in 96-well plates at 5000 cells/well in triplicates. To measure cell viability, we added 10  $\mu$ L MTT (5 mg/mL) to each well and incubated the plates for 4 hours at 37°C. And then 100  $\mu$ L solubilization buffer was added to each well without removing medium. The plates were incubated for overnight at 37°C and the absorbance at 595 nm was measured by using a spectrophotometer. Results shown are the mean  $\pm$  standard error (SEM) of 3 independent experiments.

#### Cell cycles analysis

Cells were harvested by trypsinization and fixed in 70% ethanol at -20°C for at least overnight. The cells were then treated with 50  $\mu$ L of 100  $\mu$ g/mL boiled RNase A (Sigma, USA) for 30 min followed by staining with 200  $\mu$ L propidium iodide (from 50  $\mu$ g/mL stock solution). Cell cycle was acquired using a flow cytometry (LSR II, BD Biosciences, USA) and data was analyzed using the ModFit LT software (Verity Software House, USA). All experiments were performed three times independently.

#### Apoptosis by flow cytometry

Cell apoptosis was detected using Annexin V-FITC apoptosis detection reagent (BD, USA) according to the manufacturer's

instructions. Briefly, cells were washed twice with cell staining buffer and resuspended in binding buffer at  $1 \times 10^5$  cells/100  $\mu$ L. To 100  $\mu$ L of cell suspension, 5  $\mu$ L of Annexin V-FITC was added and cells were incubated at room temperature for 15 min followed by addition of another 400  $\mu$ L binding buffer. Before measuring samples, 8  $\mu$ L of Hoechst 33258 was added to each sample. Cell apoptosis was then detected by using a flow cytometry (LSR II, BD Biosciences, USA) and data was analyzed using the FlowJo software (FlowJo LLC, USA).

#### Western blotting

Western blot analysis for BCL2 and CCND1 levels was performed as described by Li et al. [30], with minor modifications. Briefly, cells were lysed, and the protein concentration of total cell lysates was measured by using the BCA assay (Beyotime, China). About 25  $\mu$ g of whole cell lysates were subjected to electrophoresis and then transferred to an Immobilon-P Membrane (Merck Millipore, USA). After blocked by 5% non-fat milk for 1 hour at room temperature, the membranes were incubated with rabbit anti-human BCL2 or rabbit anti-human CCND1 (both 1: 1000, Cell Signaling, USA) and mouse anti-human  $\beta$ -actin (1: 2000, Abcam, USA) for overnight at 4°C. After incubation with corresponding secondary antibodies for 1 hour, the membrane was washed 3 times with TBST, and then incubated with BeyoECL Plus chemical luminescence solution (Beyotime, China). The membrane was then imaged using a ChemiDoc XRS imaging system and analyzed using the QuantityOne software (Bio-Rad, USA).

#### Colony formation assay

For the colony formation assay, cells were seeded at 300 cells/well on 6 well plates in triplicate and maintained in complete culture medium for 12 days until obvious colonies were formed. Colonies were then fixed by 70% ethanol for 5 min and stained with Coomassie blue dye for 5 min. A colony with more than 50 cells were considered as a colony and counted.

#### Transwell migration and invasion assay

Cells were transfected with miR-365 mimics or control oligos. Then cells were resuspended in 200  $\mu$ L serum free medium and seeded in the upper part of the Transwell-inserts (8  $\mu$ m pore membranes) in the 24-well plate with 20% FBS supplemented DMEM medium placed in the lower compartment. For the Matrigel invasion assay, 50  $\mu$ L Matrigel at 300  $\mu$ g/mL was added to a 24-well Transwell insert and solidified in a 37°C incubator for 1 hour to form a thin gel layer before cells were loaded. After incubation for 24 hours, cells that passed through the membrane were fixed on the membrane using ethanol and then stained with crystal violet. The average number of cells that passed through the membrane from 15 representative fields (5 replicates per individual experiments) was counted under a phase contrast microscope.

## Luciferase reporter assay

The region of 3'UTR of the human CCND1 and BCL2 mRNA containing the miR-365 targeting site were cloned in between the XhoI(5') and NotI(3') sites in a psi-CHECK2 vector (Promega, USA). A375 cells were co-transfected with 1 µg of p3'UTR-CCND1 or p3'UTR-BCL2 or psi-CHECK2 vector and 100 nM miR-365 mimic oligos using Lipofectamine 2000 (Invitrogen, USA). Cells were harvested 24 hours after transfection and assayed by using a Dual Luciferase Reporter Assay (Promega, USA) according to the manufacturer's instructions. The assay was performed in triplicates. The expression level of CCND1 and BCL2 3'UTR was defined as Renilla luciferase activity normalized to firefly luciferase activity for each well.

## Bioinformatics analysis

The targets genes of miR-365 were predicted using the miRanda, DIANA-microT and TargetScan database and the predicted targets that showed up in at least 2 databases were selected for further analysis. To further investigate the functional roles of miR-365, target genes were subjected to Gene Ontology (GO) analysis and Kyoto Encyclopedia of Genes and Genomes (KEGG) pathway enrichment analysis using DAVID Bioinformatics Resources [31].

## Analysis of TCGA melanoma dataset

Skin Cutaneous Melanoma (SKCM) dataset for 470 melanoma samples was obtained from The Cancer Genome Atlas (TCGA). Level 3 miRNA-Seq data generated from the miSeq Illumina platform and clinicopathological features of patients were retrieved from the TCGA Data Portal (released on 04/08/16). All samples had clinical and follow-up information. The dataset contained 448 patients with miRNA-Seq data, therefore only patients with miRNA data were used in this analysis. As the data were obtained from TCGA, further approval by an ethics committee was not required. This study meets the publication guidelines provided by TCGA. Expression of miR-365 in patients at different disease stages was compared by using one-way ANOVA. Overall survival (OS) and disease-free survival (DFS) were assessed by using the Kaplan-Meier method and curves were compared by univariate (log-rank) test.

## Statistical analysis

Statistical analysis was performed using the GraphPad Prism 6 (GraphPad Software Inc., USA). The difference between 2 groups was analyzed by Student's *t*-test; the means of more than 2 groups were compared by using one-way ANOVA followed by the Tukey-Kramer method. Each experiment was repeated at least 3 times and data was presented as mean ± SEM. A *P* value ≤ 0.05 was considered to be significant.

## Results

### MiR-365 inhibited cell proliferation and induced apoptosis in melanoma

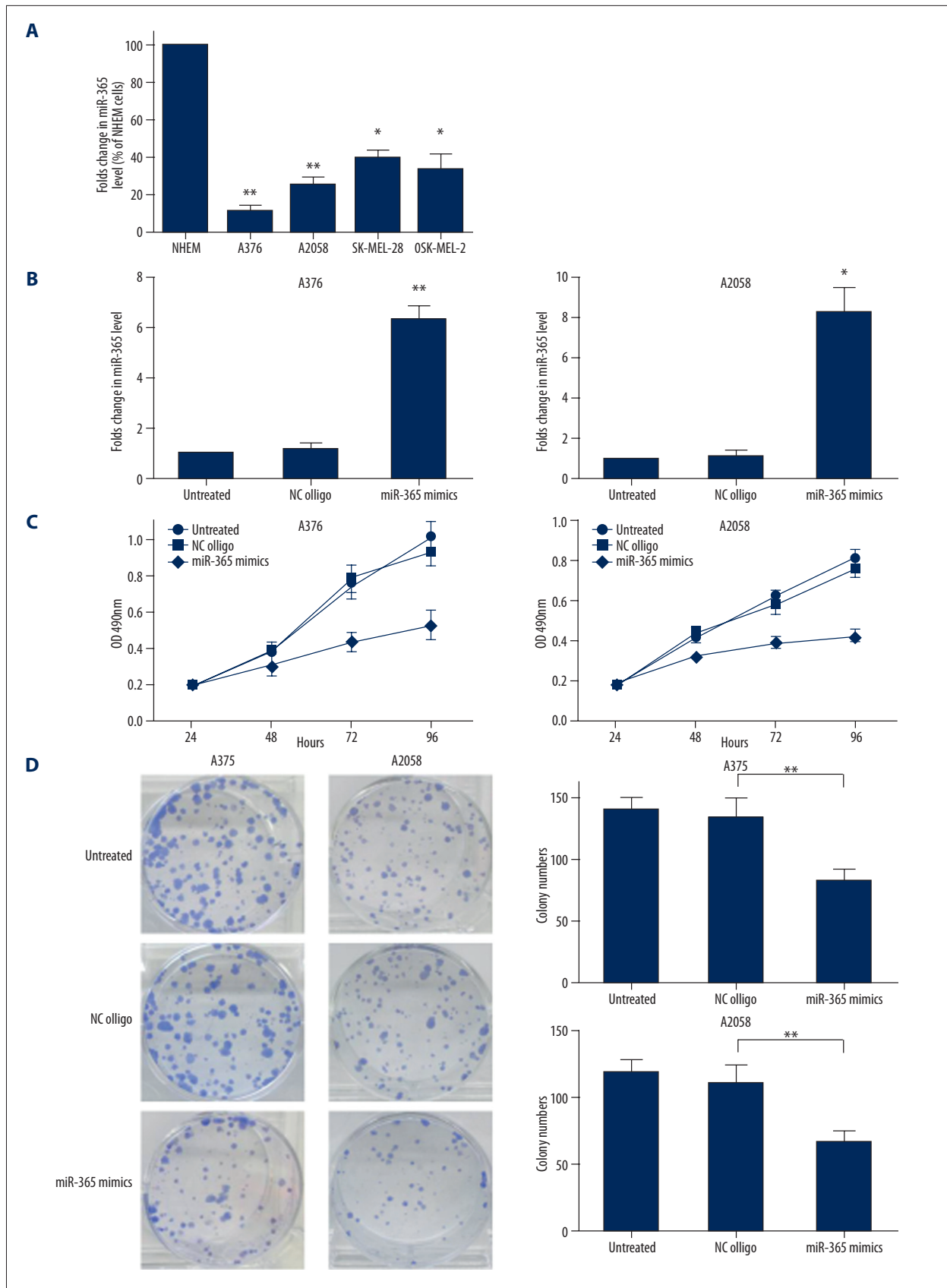
Initially, we found out that miR-365 was downregulated in 4 melanoma cell lines, A375, A2058, SK-MEL-2, and SK-MEL-28 compared to a melanocyte cell line, NHEM (Figure 1A). We then investigated the biological functions of miR-365 in melanoma cell lines. MiR-365 was overexpressed in A375 and A2058 melanoma cell lines by transient transfection of a miR-365 mimic oligo, and the overexpression of miR-365 was validated by qRT-PCR (Figure 1B). The results of MTT assays revealed that ectopic expression of miR-365 significantly reduced cell viability in both A375 and A2058 cells (Figure 1C). We then explored the potential mechanisms for the decreased cell viability in miR-365 overexpressing cells. The colony formation assay indicated that melanoma cells overexpressing miR-365 has decreased proliferation ability than the control cells (Figure 1D). The cell cycle analysis showed a significant increase in population at the G0/G1 phase and a decrease in the population at S phase (Figure 1E), suggesting a G1/S blockage was caused by miR-365 overexpression. In addition, we also found that miR-365 led to a substantial increase in cell apoptosis (Figure 1F). Together, these results indicated that miR-365 played a tumor suppressive role in melanoma likely through inhibiting cell proliferation, blocking cell cycle progression and enhancing cell apoptosis.

### miR-365 suppressed melanoma migration and invasion

Bai et al. reported that miR-365 levels were inversely correlated with melanoma metastasis [13]. We therefore investigated the effects of miR-365 overexpression on the migration and invasion abilities of A375 and A2058 melanoma cells. The Transwell migration assay and Matrigel invasion assay indicated that overexpression of miR-365 significantly suppressed melanoma cell migration (Figure 2A) and invasion (Figure 2B) capacities, respectively.

### miR-365 targeted BCL2 and CCND1

Both BCL2 and CCND1 were reported as direct targets of miR-365 in colon cancer [11]. However, these regulatory associations have not been established in melanoma and the roles of BCL2 and CCND1 in miR-365-mediated phenotypes in melanoma have not been studied. Thus, we examined the effects of miR-365 overexpression on the endogenous mRNA and proteins levels of BCL2 and CCND1 in A375 and A2058 melanoma cells. As expected, mRNA (Figure 3A) and protein levels (Figure 3B) of BCL2 and CCND1 were significantly downregulated in cells overexpressing miR-365 compared to control cells. To investigate whether BCL2 and CCND1 were direct targets



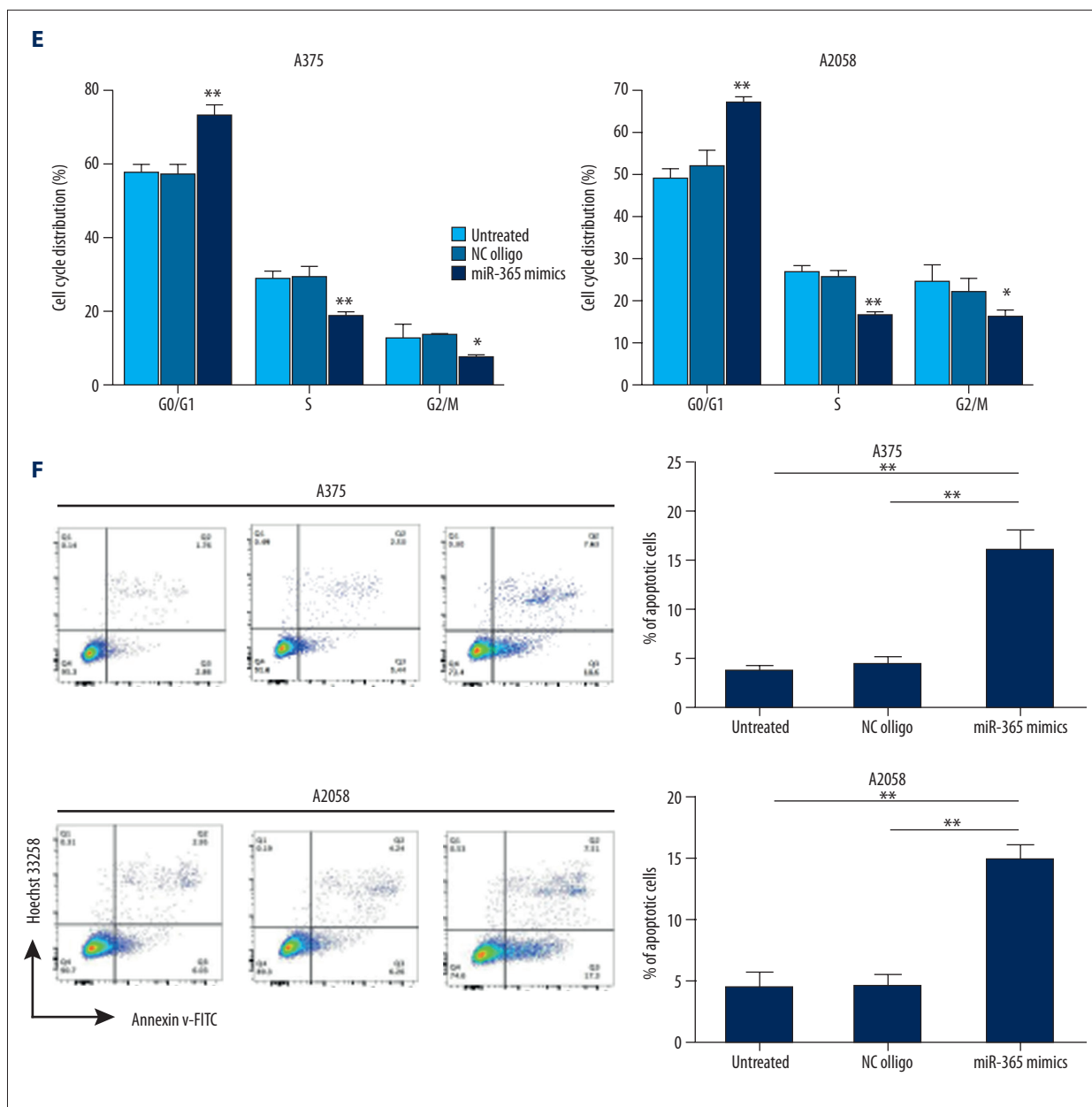


**Figure 1.** MiR-365 inhibited cell proliferation and induced apoptosis in melanoma. (A) The expression of miR-365 was measured in melanocytes and 4 melanoma cell lines, A375, A2058, SK-MEL-2, and SK-MEL-28 by qRT-PCR. A375 and A2058 were transfected with 100 nM miR-365 mimics or control oligos for 48 hours. (B) The expression levels of miR-365 were measured by qRT-PCR. (C) The cell viability was measured by MTT assay. (D) The colony formation assay was performed to analyze the effects of miR-365 on cell proliferation. In each well of a 6 well plate, 300 cells were plated and incubated for 10–12 days until colonies were visible. Cell cluster with over 50 cells was counted as a colony. (E) Cell cycle was analyzed by using PI staining flow cytometry. (F) Cell apoptosis was measured by using Annexin V-FITC/Hoechst 33258 double staining flow cytometry. Data shown are the mean ±SEM of 3 independent experiments. \*  $P < 0.05$ , \*\*  $P < 0.01$ , and ns, no significance.

of miR-365 in melanoma we constructed luciferase reporter plasmids containing parts of BCL2 and CCND1 3'UTR with either a wildtype or deleted miR-365 target sites (Figure 3C). As shown by the results of luciferase reporter assays, co-transfection of miR-365 suppressed the luciferase activity of the

reporters containing wild-type miR-365 target sites of BCL2 and CCND1 but not that of the reporters containing deleted miR-365 target sites in A375 cells (Figure 3D), indicating that both BCL2 and CCND1 were directly regulated by miR-365 in melanoma cells.

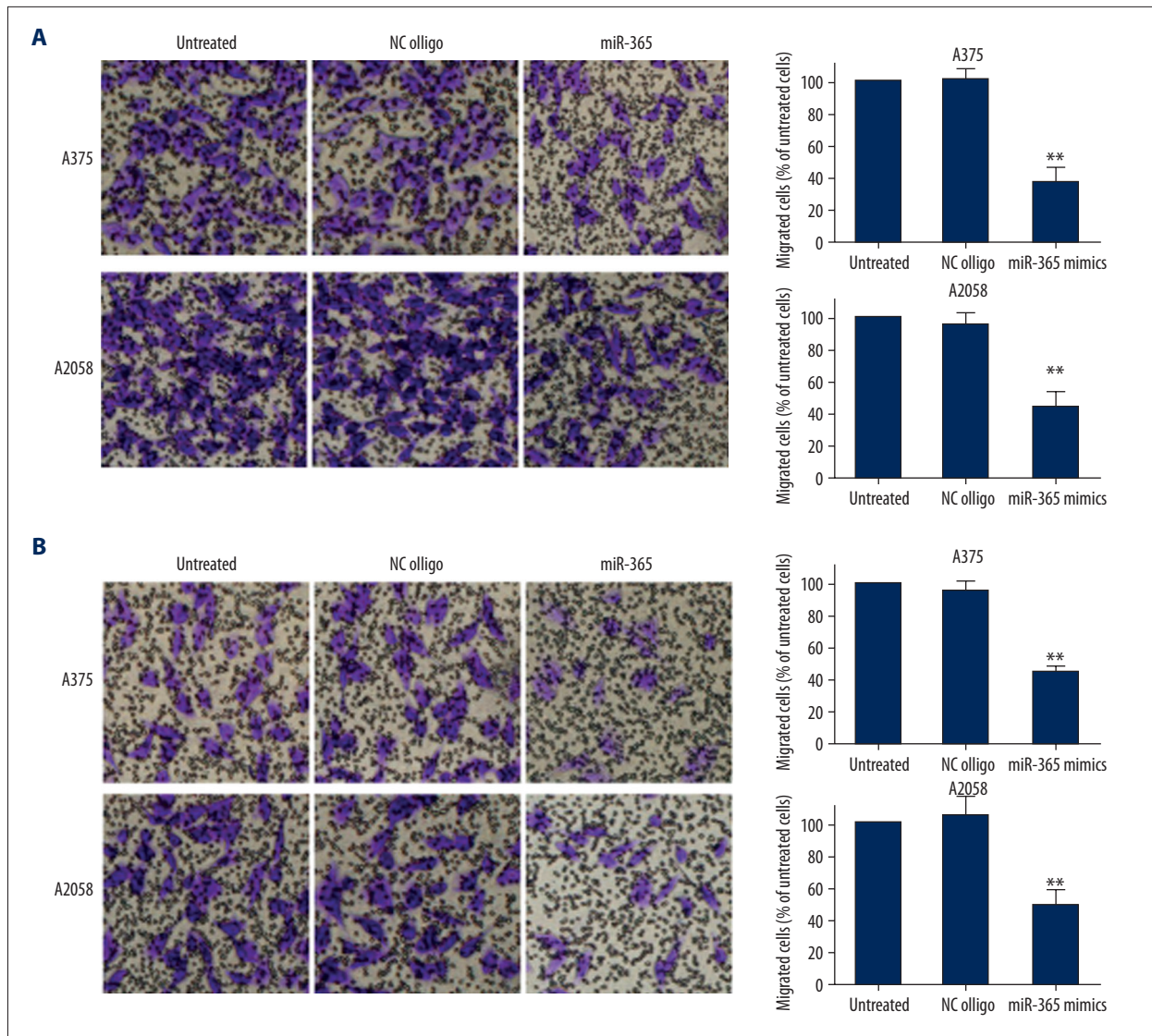


**Figure 2.** MiR-365 suppressed melanoma migration and invasion. **(A)** The effects of miR-365 on cell migration was measured using the Transwell assays. **(B)** The Transwell Matrigel invasion assay was used to assess the effects of miR-365 on invasion capacity of cells. In both assays, cells were seeded in the upper chamber of the Transwell (8  $\mu$ m pore) set and attracted to migrate through the membrane. In the invasion assay, 50  $\mu$ L Matrigel at 300  $\mu$ g/mL was added to form a thin gel layer before the assay. Cells that passed through the membrane were fixed on the membrane using methanol and stained with crystal violet and the number of migrated cells was quantified. Data shown are the mean  $\pm$ SEM of 3 independent experiments. \*  $P < 0.05$ , \*\*  $P < 0.01$ , and ns, no significance.

### The effects of miR-365 were partially mediated through targeting CCND1 and BCL2

To investigate the role of CCND1 in miR-365-induced cell cycle arrest, we co-transfected A375 and A2058 cells with miR-365 mimic oligos and a construct encoding CCND1 or an empty vector. We found out that restoration of CCND1 levels eliminated the effects of miR-365 overexpression on cell cycle arrest in both cell lines (Figure 4A). To investigate the role of BCL2 in miR-365-induced cell apoptosis, we co-transfected

A375 and A2058 cells with miR-365 mimic oligos and a construct coding BCL2 or an empty vector. The results revealed that co-transfection of miR-365 mimics with BCL2 expressing plasmid led to significant reduction in apoptotic rate in both cell lines (Figure 4B). These data suggested that the anti-tumor effects of miR-365 were at least partially mediated by inhibition of its target genes, BCL2 and CCND1.

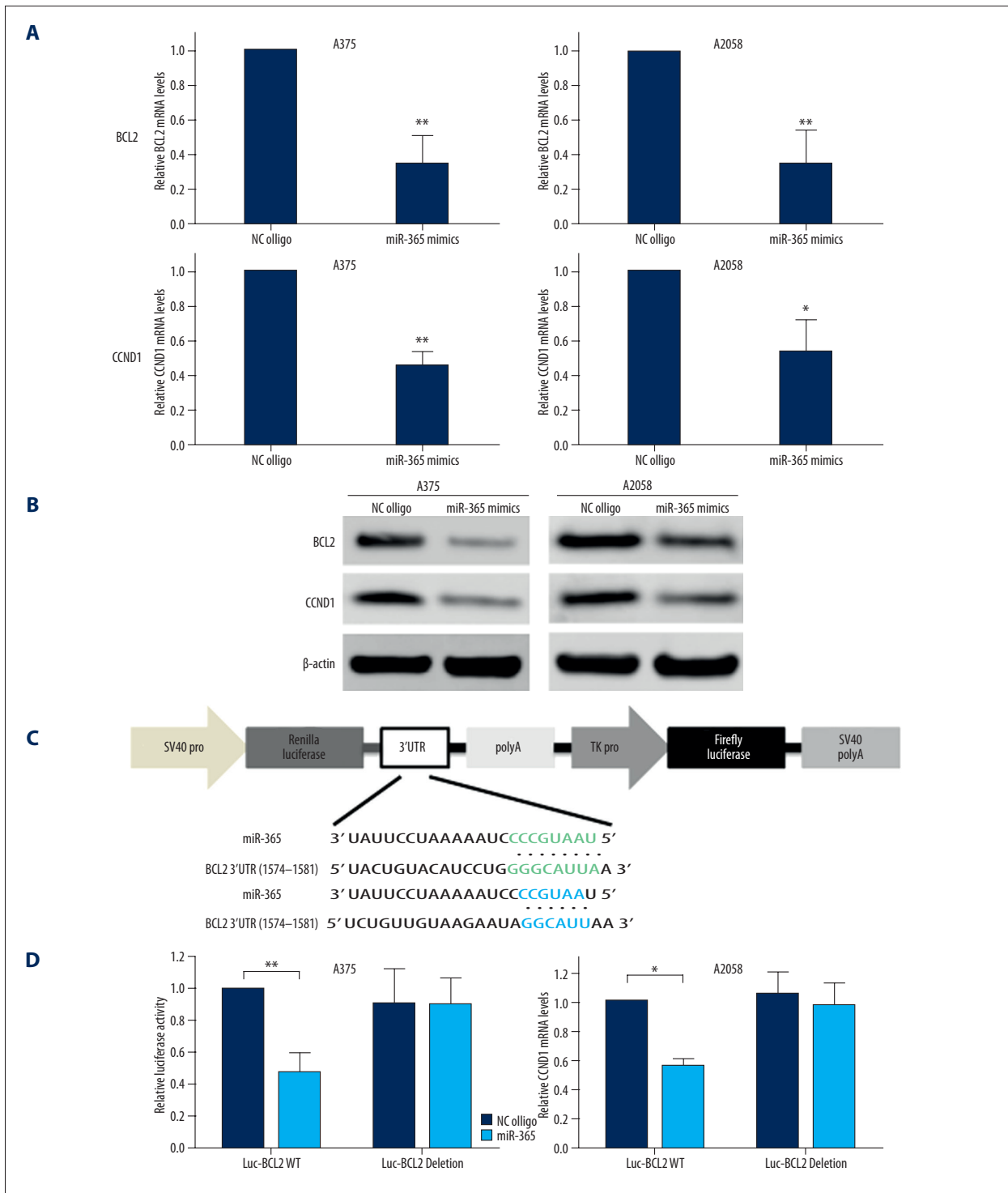


**Figure 3.** MiR-365 targeted BCL2 and CCND1. A375 and A2058 were transfected with 100 nM miR-365 mimics or control oligos for 48 hours. **(A)** mRNA levels of BCL2 and CCND1 were measured by qRT-PCR. **(B)** Protein levels of BCL2 and CCND1 were measured using western blot. **(C)** An illustration of the targeting sites of miR-365 on 3'UTR of BCL2 and CCND1 and the constructs of the luciferase reporter plasmids. **(D)** The dual-luciferase reporter assay was performed to show that BCL2 and CCND1 were directly targeted by miR-365. A375 cells were co-transfected with indicated oligos and constructs. The Renilla and firefly luciferase activity was then measured using the dual-luciferase kit as instructed by the manufacture's protocol. Data shown are the mean  $\pm$ SEM of three independent experiments. \*  $P < 0.05$ , \*\*  $P < 0.01$ , and ns, no significance.

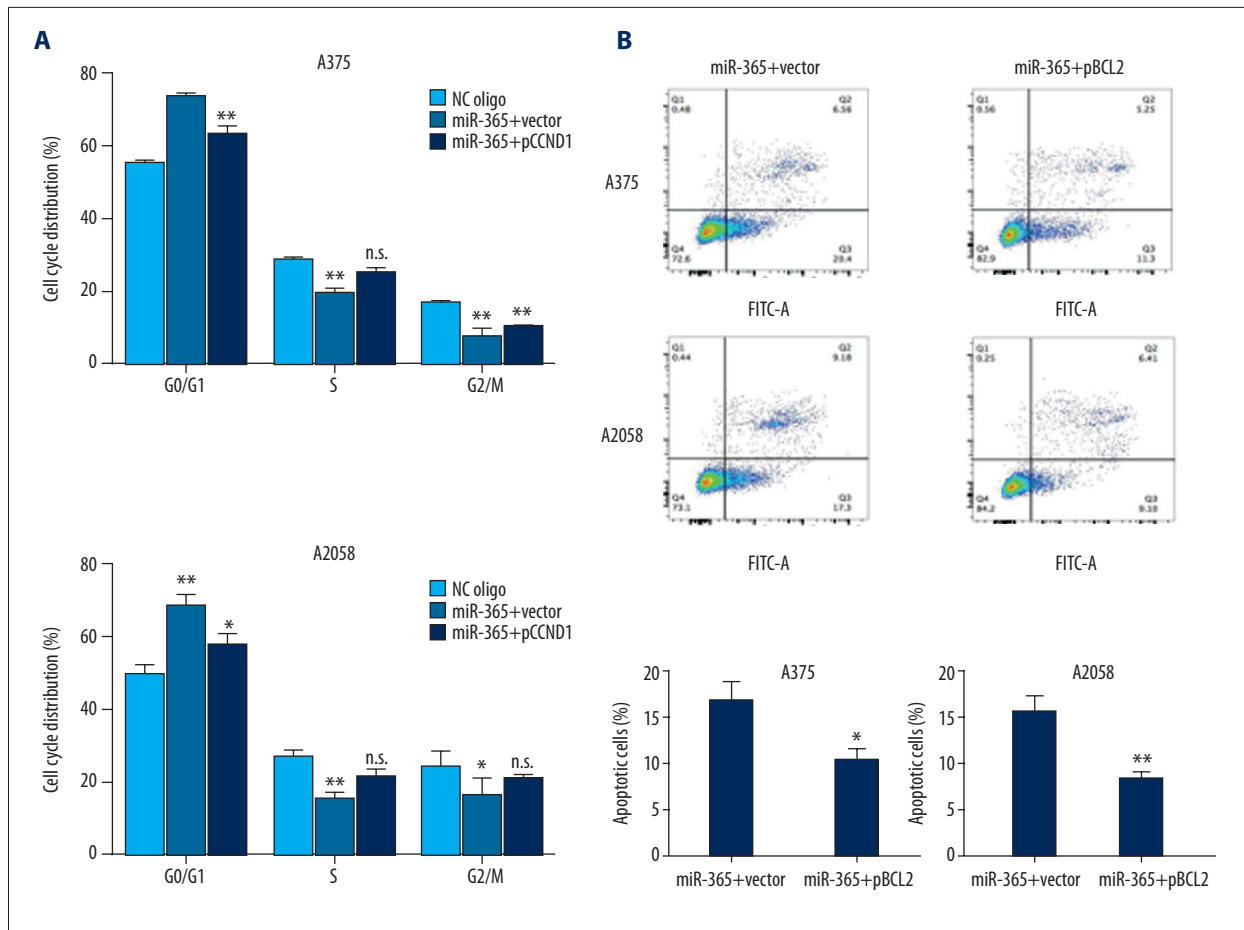


**Figure 4.** The effects of miR-365 were partially mediated through targeting BCL2 and CCND1. (A) A375 and A2058 cells were co-transfected with miR-365 mimic oligos and a construct encoding CCND1 or an empty vector. Cell cycle was analyzed using the PI staining flow cytometry. (B) A375 and A2058 cells were co-transfected with miR-365 mimic oligos and a construct encoding BCL2 or an empty vector. Cell apoptosis was measured by using Annexin V-FITC/Hoechst 33258 double staining flow cytometry. Data shown are the mean  $\pm$ SEM of 3 independent experiments. \*  $P < 0.05$ , \*\*  $P < 0.01$ , and ns, no significance.

### GO analysis and KEGG pathway enrichment analysis

To gain further insight into the cellular functions of miR-365, the predicted target genes of miR-365 were retrieved using the miRanda, DIANA-microT and TargetScan database (Figure 5) and subjected to GO analysis and KEGG pathway enrichment analysis. The GO function enrichment analysis explored the functional roles of miR-365 target genes in terms of biological processes, cellular components and molecular functions. The top enriched biological processes were associated with “regulation of gene transcription” (Table 1); the top enriched cell components included “nucleus”, “nucleoplasm”, and “neuron projection” (Table 2); the top enriched molecular functions were involved in “sequence-specific DNA binding”, “transcriptional activator activity” and “protein binding” (Table 3). KEGG pathway enrichment analysis was also performed to identify significant pathways enriched in miR-365 target genes. KEGG analysis indicated that these genes were mainly involved in

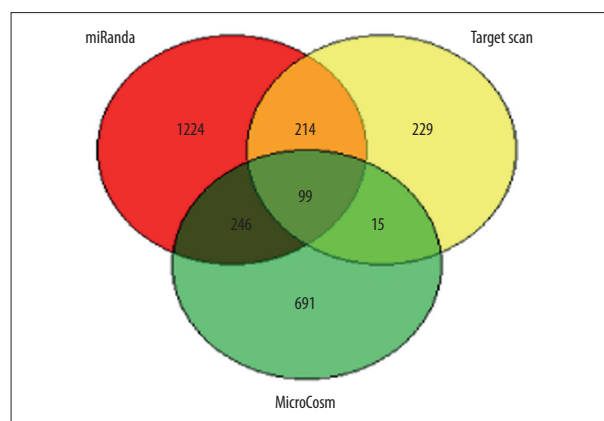


**Figure 5.** The predicted target genes of miR-365. The predicted target genes of miR-365 were retrieved using the miRanda, DIANA-microT and TargetScan database and the genes showed up in at least 2 databases were subjected to GO and KEGG analysis.

**Table 1.** The top 10 enriched biological processes in the GO functional analysis.

GO category	GO term	Gene number	P-value
GOTERM_BP	Positive regulation of transcription from RNA polymerase II promoter	58	2.90E-09
GOTERM_BP	Transcription, DNA-templated	84	7.50E-07
GOTERM_BP	Positive regulation of transcription, DNA-templated	32	6.50E-06
GOTERM_BP	Neuron migration	13	1.40E-05
GOTERM_BP	Positive regulation of sodium ion transport	6	1.10E-04
GOTERM_BP	Axon guidance	14	2.10E-04
GOTERM_BP	Transcription from RNA polymerase II promoter	28	2.70E-04
GOTERM_BP	Small GTPase mediated signal transduction	17	5.30E-04
GOTERM_BP	Negative regulation of cell migration	10	6.70E-04
GOTERM_BP	Regulation of transcription, DNA-templated	59	6.80E-04

**Table 2.** The top 10 enriched cell components in the GO functional analysis.

GO category	GO term	Gene number	P-value
GOTERM_CC	Nucleus	175	3.50E-05
GOTERM_CC	Nucleoplasm	101	5.80E-05
GOTERM_CC	Neuron projection	17	5.50E-04
GOTERM_CC	Cytoplasmic, membrane-bounded vesicle	11	2.50E-03
GOTERM_CC	Cell-cell junction	12	3.60E-03
GOTERM_CC	Intracellular	51	3.80E-03
GOTERM_CC	Transcription factor complex	13	4.10E-03
GOTERM_CC	NuA4 histone acetyltransferase complex	4	9.30E-03
GOTERM_CC	Cytosol	105	1.00E-02
GOTERM_CC	Membrane	72	1.20E-02

cancer-related pathways, Rap1 signaling pathway, and phosphatidylinositol signaling system (Table 4).

#### miR-365 was not correlated with clinicopathological stage and survival of melanoma patients

We then analyzed the SKCM datasets in TCGA for correlation between miR-365 level and clinicopathological stage and the survival of melanoma patients. The results revealed that miR-365 level was not obviously different among patients at different T stage ( $P>0.05$ , Figure 6A), N stage ( $P>0.05$ , Figure 6B), M stage ( $P>0.05$ , Figure 6C) and overall clinicopathological stage ( $P>0.05$ , Figure 6D). Furthermore, Kaplan-Meier analysis failed to discover significant differences in OS and DFS between patients with high and low miR-365 levels ( $P>0.05$ , Figure 6E).

## Discussion

Investigation into the molecular mechanisms responsible for melanoma carcinogenesis and progression, especially the exploration of dysregulated miRNAs in melanoma, represents a popular and promising field of study and is essential for developing novel therapeutics.

MiR-365 is located in the chromosome region 16p13.12. The expression pattern of miR-365 is cancer type-dependent. MiR-365 was highly expressed in cutaneous squamous cell carcinoma [8,9], breast cancer [32], and invasive pancreatic ductal adenocarcinoma [10]. In contrast, miR-365 was downregulated in colon cancer [11] and lung cancer [12]. The function of miR-365 is complicated, it may function as a tumor suppressor or an oncogene depending on the cancer types. For example, miR-365 was reported to suppress cell cycle progression

**Table 3.** The top 10 enriched molecular functions in the GO functional analysis.

GO category	GO term	Gene number	P-value
GOTERM_MF	Sequence-specific DNA binding	34	1.80E-06
GOTERM_MF	RNA polymerase II core promoter proximal region sequence-specific DNA binding	27	1.80E-06
GOTERM_MF	Transcriptional activator activity, RNA polymerase II core promoter proximal region binding	19	3.50E-05
GOTERM_MF	Protein binding	198	6.90E-05
GOTERM_MF	Transcription factor activity, sequence-specific dna binding	45	1.50E-04
GOTERM_MF	Chromatin binding	23	5.90E-04
GOTERM_MF	Enzyme binding	20	9.90E-04
GOTERM_MF	DNA binding	65	1.20E-03
GOTERM_MF	Phosphatidylinositol binding	9	1.50E-03
GOTERM_MF	Zinc ion binding	48	2.30E-03

**Table 4.** The top 10 enriched signaling pathways in the KEGG analysis.

KEGG category	KEGG term	Gene number	P-value
KEGG_PATHWAY	Rap1 signaling pathway	16	3.00E-04
KEGG_PATHWAY	Pathways in cancer	23	4.10E-04
KEGG_PATHWAY	Hepatitis B	12	1.20E-03
KEGG_PATHWAY	Prostate cancer	9	1.80E-03
KEGG_PATHWAY	Chronic myeloid leukemia	8	2.30E-03
KEGG_PATHWAY	Phosphatidylinositol signaling system	9	3.50E-03
KEGG_PATHWAY	Estrogen signaling pathway	9	3.70E-03
KEGG_PATHWAY	Renal cell carcinoma	7	6.10E-03
KEGG_PATHWAY	Cholinergic synapse	9	7.40E-03
KEGG_PATHWAY	B cell receptor signaling pathway	7	8.20E-03

and promote apoptosis of colon cancer cells by probably targeting Cyclin D1 and Bcl-2 [11,33]; miR-365 expression levels were reduced in lung cancer tissues and ectopic miR-365 expression could inhibit cell proliferation of lung cancer cell lines by targeting thyroid transcription factor 1 (TTF-1), which is an essential factor in lung developmental and a prognostic marker for non-small cell lung cancer. However, miR-365 was rarely studied in melanoma. In the only literature studying miR-365 in melanoma, Bai et al. found that the expression of miR-365 was significantly downregulated compared with that in matched normal tissue [13] and overexpression of miR-365 inhibited growth, invasion and metastasis of malignant melanoma through targeting neuropilin1 (NRP1). Therefore, we carried out the present study to further explore the roles of miR-365 in melanoma.

In this study, we initially found that miR-365 expression was lower in melanoma cells compared with non-transformed melanocyte (Figure 1A). And the levels of miR-365 was not relevant to the status of BRAF mutation, as it was significantly decreased in both BRAF wildtype cell lines, A375, A2058, and SK-MEL-28, and in BRAF mutant cell lines, SK-MEL-2. Next, we found that overexpression of miR-365 led to significant decrease in cell viability (Figure 1C). Investigation into the underlying mechanism showed that ectopic expression of miR-365 remarkably suppressed clonogenic capacity and induced cell cycle arrest and apoptosis in melanoma cell lines (Figure 1D–1F). In addition, miR-365 significantly compromised the migration and invasion capacities of melanoma cell *in vitro* (Figure 2A, 2B). These results were in consistence with Bai et al. study in melanoma and suggested that miR-365 functioned as a tumor suppressor in melanoma.

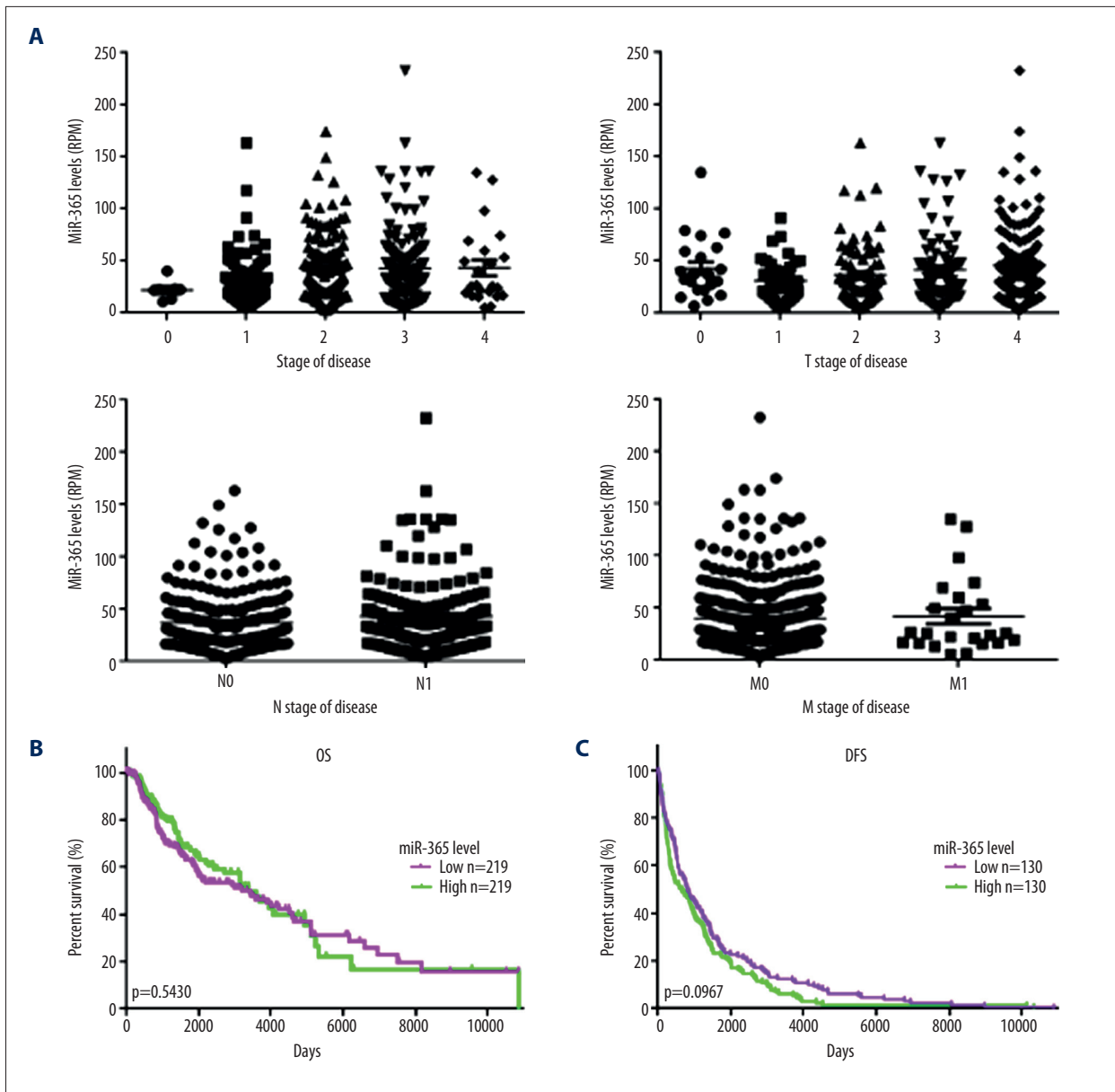


**Figure 6.** MiR-365 was not correlated with clinicopathological stage and survival of melanoma patients. The miRNA-Seq and clinical data from the TCGA SKCM datasets were obtained. **(A)** The expression levels of miR-365 among different clinicopathological stage were compared using one-way ANOVA. **(B)** Overall survival and **(C)** Disease-free survival were assessed by the Kaplan-Meier method and curves were compared by using the log-rank test. Significance was defined as  $P < 0.05$ .

Regarding the target genes of miR-365, a variety of genes have been reported, including CCND1, BCL2, NRP1, TTF-1. Among these genes, CCND1 is considered as an important proliferation-promoting molecule; BCL2 is a fundamental anti-apoptotic gene with a recognized role in cancer development (Figure 4D). However, this regulatory association has not been reported in melanoma. We found that overexpression of miR-365 downregulated the mRNA and protein levels of these 2 genes in A375 and A2058 cell lines (Figure 4A, 4B). To confirm that CCND1 and BCL2 are direct targets of miR-365,

we performed a luciferase reporter assay, showing that CCND1 and BCL2 were directly targeted by miR-365 in melanoma cells (Figure 4E). Finally, to explore the roles of CCND1 and BCL2 in miR-365-mediated cell cycle arrest and apoptosis, we co-transfected melanoma cells with miR-365 mimic oligos and a construct encoding either CCND1 or BCL2. The results revealed that restoration of CCND1 or BCL2 attenuated the effects of miR-365 overexpression on cell cycle and apoptosis, respectively (Figure 5A, 5B). Our result was consistent with Nie et al. study which has shown that BCL2 and CCND1 are direct

targets of miR-365 in colon cancer and that knockdown of the endogenous CCND1 or BCL2 was able to mimic the effect of miR-365 [11]. Together, these results suggested that miR-365 probably is a novel tumor suppresser in melanoma through targeting CCND1 and BCL2, as well as other potential targets. We should notice that the regulatory network by miRNAs is very complicated. One gene is regulated by multiple miRNAs, and a specific miRNA can regulate multiple genes. Therefore, other target genes in addition to CCND1 and BCL2 may also participate in the functions of miR-365.

This notion highlighted the need for further studies to reveal the entire “targetome” of miR-365 in the development of melanoma. To gain further insight into the cellular functions of miR-365, we then performed the GO functional enrichment analysis and KEGG pathway enrichment analysis for the predicted target genes of miR-365 retrieved from the miRanda, DIANA-microT and TargetScan database. GO function enrichment analysis revealed that the most prominent functions of miR-365 target genes were involved in regulation of gene transcription. KEGG pathway enrichment analysis indicated that miR-365 target genes were mainly involved in cancer-related pathways. Thus, analysis of the “targetome” of miR-365 further revealed the association of miR-365 with cancer and dysregulated gene transcription may contribute to the function of miR-365.

We then analyzed the TCGA SKCM dataset for correlation between miR-365 levels and clinicopathological stage or the prognosis of melanoma patients. The results revealed that miR-365 levels were not obviously different among patients with different T stage, N stage, M stage, and overall clinicopathological

stage (all  $P>0.05$ , Figure 5A). Furthermore, Kaplan-Meier analysis failed to discover significant difference in OS and DFS between patients with high and low miR-365 levels (both  $P>0.05$ , Figure 5B, 5C). The prognosis of patients can be influenced by many factors, such as disease stage and treatment. Mir-365 is just one of the many factors, therefore, its effect on patient outcome may be covered or counteract by the effect of other factors, although miR-365 showed obvious biological effects in melanoma cell lines. The discrepancy between *in vitro* and *in vivo* data again highlighted the complexity of miRNA regulatory network and further studies are guaranteed to completely understand the roles miR-365 in melanoma development.

## Conclusions

In sum, our data suggested that miR-365 was downregulated in melanoma cells and played a tumor suppressive role in melanoma development through regulating multiple target genes that are essential to key cellular functions, such as cell proliferation, apoptosis, migration, and invasion. However, the TCGA data failed to discover the association of miR-365 with progression and development of melanoma patients. Further studies in animal models and human samples are required for the full understanding of the roles miR-365 in melanoma development.

## Conflict of interest

None.

## Reference:

1. Crawford AB, Nessim C, Weaver J, van Walraven C: Wait times for melanoma surgery: Is there an association with overall survival? *Ann Surg Oncol*, 2018; 25(1): 265–70
2. Siegel RL, Miller KD, Jemal A: Cancer statistics, 2015. *Cancer J Clin*, 2015; 65(1): 5–29
3. Keller HR, Zhang X, Li L et al: Overcoming resistance to targeted therapy with immunotherapy and combination therapy for metastatic melanoma. *Oncotarget*, 2017; 8(43): 75675–86
4. Mansoori B, Mohammadi A, Shirjang S, Baradaran B: MicroRNAs in the diagnosis and treatment of cancer. *Immunol Invest*, 2017; 46(8): 880–97
5. Varamo C, Ocellini M, Vivenza D et al: MicroRNAs role as potential biomarkers and key regulators in melanoma. *Genes Chromosomes Cancer*, 2017; 56(1): 3–10
6. Yu X, Li R, Shi W et al: Silencing of MicroRNA-21 confers the sensitivity to tamoxifen and fulvestrant by enhancing autophagic cell death through inhibition of the PI3K-AKT-mTOR pathway in breast cancer cells. *Biomed Pharmacother*, 2016; 77: 37–44
7. Shen H, Xing C, Cui K et al: MicroRNA-30a attenuates mutant KRAS-driven colorectal tumorigenesis via direct suppression of ME1. *Cell Death Differ*, 2017; 24(7): 1253–62
8. Zhou M, Zhou L, Zheng L et al: miR-365 promotes cutaneous squamous cell carcinoma (CSCC) through targeting nuclear factor I/B (NFIB). *PLoS One*, 2014; 9(6): e100620
9. Zhou M, Liu W, Ma S et al: A novel onco-miR-365 induces cutaneous squamous cell carcinoma. *Carcinogenesis*, 2013; 34(7): 1653–59
10. Li M, Liu L, Zang W et al: miR365 overexpression promotes cell proliferation and invasion by targeting ADAMTS-1 in breast cancer. *Int J Oncol*, 2015; 47(1): 296–302
11. Nie J, Liu L, Zheng W et al: microRNA-365, down-regulated in colon cancer, inhibits cell cycle progression and promotes apoptosis of colon cancer cells by probably targeting Cyclin D1 and Bcl-2. *Carcinogenesis*, 2012; 33(1): 220–25
12. Kang SM, Lee HJ, Cho JY: MicroRNA-365 regulates NKX2-1, a key mediator of lung cancer. *Cancer Lett*, 2013; 335(2): 487–94
13. Bai J, Zhang Z, Li X, Liu H: MicroRNA-365 inhibits growth, invasion and metastasis of malignant melanoma by targeting NRP1 expression. *Int J Clin Exp Pathol*, 2015; 8(5): 4913–22
14. Musgrove EA, Caldon CE, Barraclough J et al: Cyclin D as a therapeutic target in cancer. *Nat Rev Cancer*, 2011; 11(8): 558–72
15. Mohammadzadeh F, Hani M, Ranaee M, Bagheri M: Role of cyclin D1 in breast carcinoma. *J Res Med Sci*, 2013; 18(12): 1021–25
16. Gautschi O, Ratschiller D, Gugger M et al: Cyclin D1 in non-small cell lung cancer: A key driver of malignant transformation. *Lung Cancer Amst Neth*, 2007; 55(1): 1–14
17. Flørenes VA, Faye RS, Maelandsmo GM et al: Levels of cyclin D1 and D3 in malignant melanoma: Deregulated cyclin D3 expression is associated with poor clinical outcome in superficial melanoma. *Clin Cancer Res*, 2000; 6(9): 3614–20

18. Katunarić M, Jurišić D, Petković M et al: EGFR and cyclin D1 in nodular melanoma: Correlation with pathohistological parameters and overall survival. *Melanoma Res*, 2014; 24(6): 584–91
19. Frenzel A, Grespi F, Chmielewski W, Villunger A: Bcl2 family proteins in carcinogenesis and the treatment of cancer. *Apoptosis*, 2009; 14(4): 584–96
20. Hata AN, Engelman JA, Faber AC: The BCL2 family: Key mediators of the apoptotic response to targeted anticancer therapeutics. *Cancer Discov*, 2015; 5(5): 475–87
21. Bakhshi A, Jensen JP, Goldman P et al: Cloning the chromosomal breakpoint of t(14;18) human lymphomas: Clustering around JH on chromosome 14 and near a transcriptional unit on 18. *Cell*, 1985; 41(3): 899–906
22. Williams MM, Cook RS: Bcl-2 family proteins in breast development and cancer: Could Mcl-1 targeting overcome therapeutic resistance? *Oncotarget*, 2015; 6(6): 3519–30
23. Chaudhary KS, Abel PD, Lalani EN: Role of the Bcl-2 gene family in prostate cancer progression and its implications for therapeutic intervention. *Environ Health Perspect*, 1999; 107(Suppl. 1): 49–57
24. Eberle J, Hossini AM: Expression and function of Bcl-2 proteins in melanoma. *Curr Genomics*, 2008; 9(6): 409–19
25. Radha G, Raghavan SC: BCL2: A promising cancer therapeutic target. *Biochim Biophys Acta*, 2017; 1868(1): 309–14
26. Zhou J, Li LU, Fang LI et al: Quercetin reduces cyclin D1 activity and induces G1 phase arrest in HepG2 cells. *Oncol Lett*, 2016; 12(1): 516–22
27. Livak KJ, Schmittgen TD: Analysis of relative gene expression data using real-time quantitative PCR and the 2(-Delta Delta C(T)) method. *Methods*, 2001; 25(4): 402–8
28. Gordanpour A, Nam RK, Sugar L et al: MicroRNA detection in prostate tumors by quantitative real-time PCR (qPCR). *J Vis Exp*, 2012; (63): e3874
29. Zhang K, Wang G, Zhang X et al: COX7AR is a stress-inducible mitochondrial COX subunit that promotes breast cancer malignancy. *Sci Rep*, 2016; 6: 31742
30. Li YH, Chen M, Zhang M et al: Inhibitory effect of survivin-targeting small interfering RNA on gastric cancer cells. *Genet Mol Res*, 2014; 13(3): 6786–803
31. Huang DW, Sherman BT, Tan Q et al: The DAVID Gene Functional Classification Tool: A novel biological module-centric algorithm to functionally analyze large gene lists. *Genome Biol*, 2007; 8(9): R183
32. Kodahl AR, Lyng MB, Binder H et al: Novel circulating microRNA signature as a potential non-invasive multi-marker test in ER-positive early-stage breast cancer: A case control study. *Mol Oncol*, 2014; 8(5): 874–83
33. Zhang P, Zheng C, Ye H et al: MicroRNA-365 inhibits vascular smooth muscle cell proliferation through targeting cyclin D1. *Int J Med Sci*, 2014; 11(8): 765–70